Laser-Plasma Ion Acceleration

Andrea Macchi

National Institute of Optics, National Research Council (CNR/INO),
Adriano Gozzini research unit, Pisa, Italy

Enrico Fermi Department of Physics, University of Pisa, Italy

Central Laser Facility Laserlab EU training weeks
Rutherford Appleton Laboratory, Didcot (UK), December 1, 2016

Outline

- The coherent (collective) acceleration paradigm (1957)
- The (re–)discovery of laser-driven proton beams (2000)
- Acceleration mechanisms: experiment & theory
  - Target Normal Sheath Acceleration (TNSA)
  - Radiation Pressure Acceleration (RPA)
  - Collisionless Shock Acceleration (CSA)

Recent ion acceleration reviews (parochial selection)

A. Macchi, M. Borghesi, M. Passoni,
Ion Acceleration by Superintense Laser-Plasma Interaction,
Rev. Mod. Phys. **85** (2013) 571

A. Macchi, A. Sgattoni, S. Sinigardi, M. Borghesi, M. Passoni,
Advanced Strategies for Ion Acceleration using High Power Lasers, Plasma Phys. Contr. Fus. **55** (2013) 124020

M. Borghesi, A. Macchi, *Laser-Driven Ion Accelerators: State of the Art and Applications*, in: *Laser-Driven Particle Acceleration Towards Radiobiology and Medicine*, ed. by A. Giulietti (Springer, 2016)

A. Macchi, *A Superintense Laser-Plasma Interaction Theory Primer* (Springer, 2013)
Chap.5 “Ion Acceleration” (for absolute beginners)

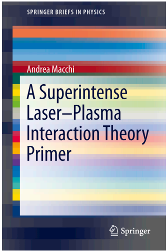

Other ion acceleration reviews

J. Schreiber, P. R. Bolton, K. Parodi,
“Hands-on” laser-driven ion acceleration: A primer for laser-driven source development and potential applications,
Rev. Sci. Instrum. **87**, 071101 (2016)

J. C. Fernández, et al,
Fast ignition with laser-driven proton and ion beams,
Nucl. Fusion **54** (2014) 054006

H. Daido, M. Nishiuchi, A. S. Pirozhkov,
Review of Laser-Driven Ion Sources and their Applications,
Rep. Prog. Phys. **75** (2012) 056401

M. Borghesi et al,
Fast Ion Generation by High-Intensity Laser Irradiation of Solid Targets and Applications,
Fusion Science and Technology **49** (2006), 412

Focused light interaction with matter: an old story

Archimedes' mirror burning Roman ships. Giulio Parigi, ab. 1600. Uffizi Gallery, *Stanzino delle Matematiche*, Florence, Italy

Leonardo da Vinci: Studies on reflection by burning mirrors. Codex Arundel (1480-1518), British Library, London.

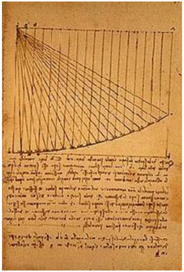

First attempts to "strongly" modify matter with intense light (heating, phase transition, ionization . . .)
Intensity of Sunlight: $I \simeq 1.4 \times 10^{-1}$ W cm^{-2}
with "ultimate" concentration $\sim 10^4 \rightarrow I \simeq 10^3$ W cm^{-2} at focus

The dawn of laser-plasma physics (1964)

"*The laser is a solution looking for a problem*" (D'Haenens to Maiman, 1960)

Q-switched lasers (1962):

10 GW on $\sim 10^{-2}$ cm spot

$\rightarrow I \simeq 10^{13}$ W cm^{-2}

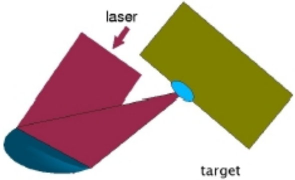

THE PHYSICS OF FLUIDS VOLUME 7, NUMBER 7 JULY 1964

On the Production of Plasma by Giant Pulse Lasers

John M. Dawson

Plasma Physics Laboratory, Princeton University, Princeton, New Jersey

(Received 10 October 1963; final manuscript received 10 March 1964)

Calculations are presented which show that a laser pulse delivering powers of the order of 10^{10} W to a liquid or solid particle with dimensions of the order of 10^{-2} cm will produce a hot plasma with temperatures in the range of several hundred eV. To a large extent the plasma temperature is held down by its rapid expansion and cooling. This converts much of the energy supplied into ordered energy of expansion. This ordered expansion energy can amount to several keV per ion. If the expanding plasma can be caught in a magnetic field and its ordered motion converted to random motion this might be utilized as a means for filling controlled thermonuclear fusion devices with hot plasma. Further, it should also be possible to do many interesting plasma experiments on such plasmas.

Race to superintense lasers

Current intensity record: $I \simeq 2 \times 10^{22}$ W cm^{-2}
[HERCULES, Michigan University, 0.3 PW, 10 fs, diffraction-limited focus $w \sim 1$ μm: Yanovsky et al, Opt. Express **16** (2008) 2109]

Some 10 PW lasers in construction:
ELI (1.5 kJ/150 fs), APOLLON (150 J/15 fs), VULCAN (300 J/30 fs) . . .
A future vision: multi-fibre laser for $I > 10^{23}$ W cm^{-2}
[Mourou et al, Nature Photonics **7** (2013) 258]

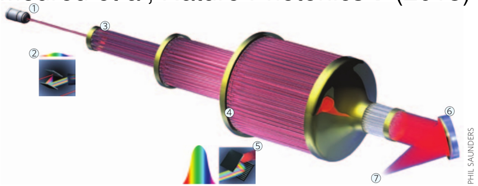

Figure 1 | Principle of a coherent amplifier network. An initial pulse from a seed laser (1) is stretched (2), and split into many fibre channels (3). Each channel is amplified in several stages, with the final stages producing pulses of ~1 mJ at a high repetition rate (4). All the channels are combined coherently, compressed (5) and focused (6) to produce a pulse with an energy of >10 J at a repetition rate of ~10 kHz (7).

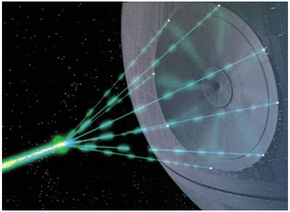

Multi-MeV protons from solid targets (2000)

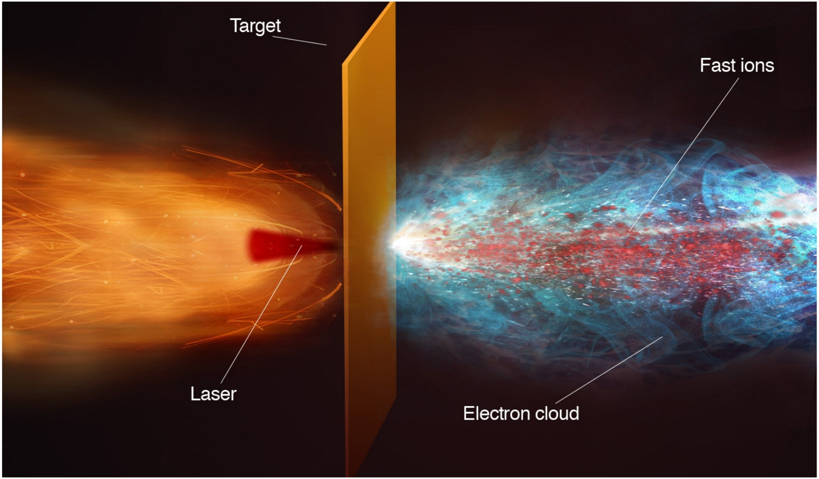

Multi-MeV protons from solid targets (2000)

Up to 58 MeV protons observed at LLNL (Livermore) Petawatt

Snavely et al, PRL **85** (2000) 2945

Other observations:

Clark et al, PRL **84** (2000) 670

Maksimchuk et al, PRL **84** (2000) 4108

Protons have been observed and characterized in many laboratories and different laser-target conditions

Max proton energy vs laser irradiance from experiments: figure from Borghesi et al, Plasma Phys. Contr. Fus. **50** (2008) 124040

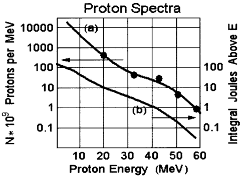

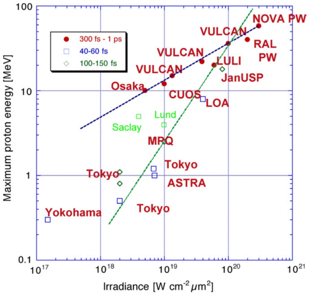

Properties of laser-accelerated protons

- in metallic targets proton originate from H impurities
- mostly broad energy spectra (exponential-like)
- large numbers - up to $\sim 2 \times 10^{13}$ protons, ~kA current
  Snavely et al, PRL **85** (2000) 2945
- charge neutralization by comoving electrons ("plasma beam")
- good collimation with energy-dependent spread $\sim 10° \div 30°$
- low emittance $\sim 4 \times 10^{-3}$ mm mrad (with cautious definition for broadband spectra)
  Nuernberg et al., Rev. Sci. Instrum. **80** (2009) 033301
- ultrashort duration: 3.5 ± 0.7 ps measured with TARANIS laser (600 fs pulse)
  Dromey et al., Nature Comm. **7** (2016) 10642

Interest in multi-MeV protons

Energy deposition dominated by Bragg peak: optimal for localized heating of matter

figure from:
U. Amaldi, G. Kraft,
Rep. Prog. Phys. **68** (2005) 1861

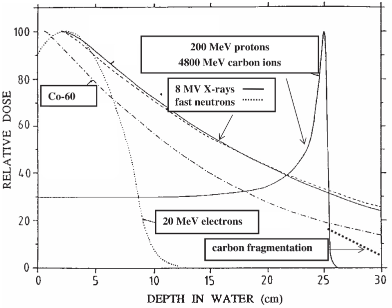

Foreseen applications:
- oncology: hadrontherapy, ion beam therapy
- triggering of nuclear reactions, isotope production
- production of warm dense matter
- diagnostic of materials
- ultrafast probing of electromagnetic fields

What is the acceleration mechanism?

The "black box" hinders the acceleration physics (not clear at discovery)
The acceleration mechanisms are of collective (cooperative, coherent) nature, based on self-consistent, non-linear plasma dynamics (complex and difficult to control)

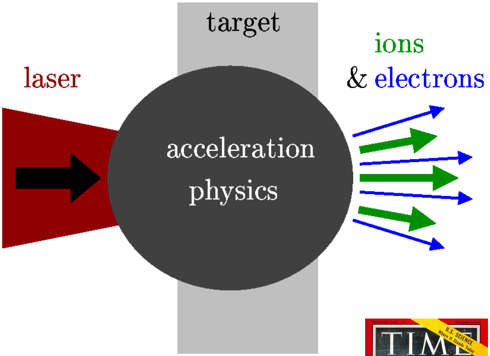

"*Is plasma involved? It can't work*"
(Edward Teller on an early proposal of controlled fusion)

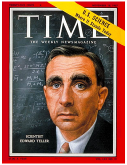

The vision of “coherent” acceleration: Veksler (1957)

The principles of coherent acceleration
V. I. Veksler, At. Energ. **2** (1957) 525
realized in laser-plasma ion acceleration

- the accelerating field on each particle is proportional to the number of accelerated particles (the higher the number, the higher the energy)
- automatic synchrony between the particles and the accelerating field
- field localization in the region where the particles are
- acceleration of quasi-neutral (charge-neutralized) bunches with large numbers of particles

Very basic ways of accelerating ions using a laser

(direct acceleration of single ions excluded)

- heat the target up to high temperatures: the laser-produced plasma will expand converting thermal energy into kinetic energy
- transfer the electromagnetic momentum flow (aka radiation pressure) of the laser pulse to the target, like the wind boosts a sail
- generate a travelling force parallel to the propagation direction, e.g. a shock wave

the basic mechanisms (TNSA, RPA, CSA) are based on the dominance of each of these three effects, respectively

(the actual mechanism in an experiment may combine all these effects)

Target Normal Sheath Acceleration (TNSA)

Physics: electric field generation by a cloud of energetic "fast" electrons leaving the rear surface of the target

The field in the charge separation region (sheath) back-holds electrons and accelerates ions

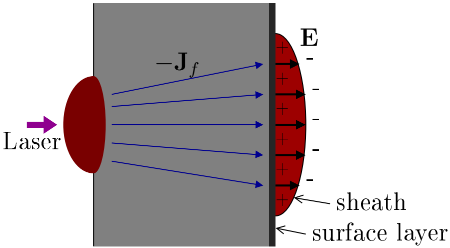

$\mathbf{J}_f$: fast electron current

Protons mostly originate from a surface impurity layer at the rear: their acceleration is favored by the initial position (at the peak of the sheath field) and the highest charge-to-mass (Z/A) ratio

Fast electron generation: a simplified picture

Needs laser-driven push-pull of electrons across the density gradient

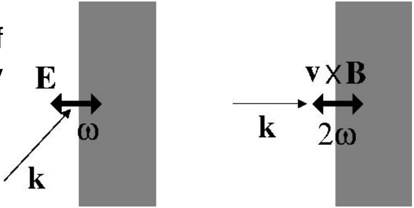

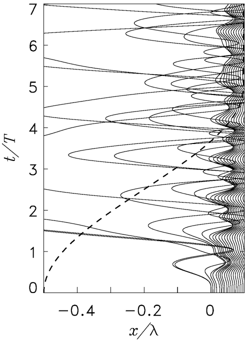

Electrons perform “half-oscillations” in vacuum and re-enter in the plasma with approximately the “quiver” energy

Oscillations driven by:
- $\mathbf{E}$ for P–polarization
- $\mathbf{v} \times \mathbf{B}$ for S–polarization or normal incidence

Fast electron generation: typical parameters

- Typical energy ("ponderomotive scaling")

$$\mathcal{E}_f = m_e c^2(\gamma - 1) \sim m_e c^2 \left(\sqrt{1 + a_0^2/2} - 1\right)$$

a_0: "relativistic" amplitude parameter

$$a_0 = \left(\frac{I\lambda^2}{10^{18}\ \text{W/cm}^2}\right)^{1/2} = \frac{eE_L}{m_e\omega c} = \frac{p_{\text{osc}}}{m_e c}$$

- conversion efficiency $\eta_f \simeq 10^{-2} - 10^{-1}$
- density $n_f \simeq 10^{20} - 10^{21}\ \text{cm}^{-3}$
- current density $\sim 10^{12}\ \text{A/cm}^2 \rightarrow 10\ \text{MA}$ over the laser spot

Static modeling of TNSA

Assume fast electrons in Boltzmann equilibrium with density n_e and temperature T_e as the only parameters to evaluate sheath extension L_s and potential drop $\Delta\Phi$

$$L_s \simeq \lambda_D = (T_e/4\pi e^2 n_e)^{1/2}, \qquad \Delta\Phi \simeq T_e/e$$

Energy gain by a "test" ion in the static sheath:

$$\mathscr{E}_{\text{max}} = Ze\Delta\Phi \simeq ZT_e$$

⚠ : exact treatment yields

$$L_s \to \infty \qquad \Delta\Phi \to \infty$$

if Boltzmann's distribution is not "truncated" at high energy

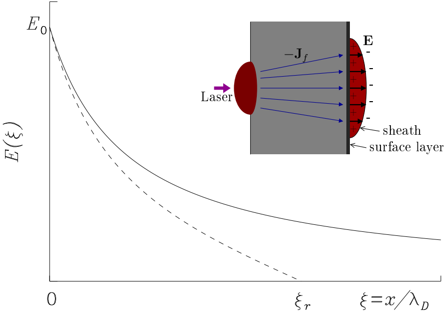

Dynamic modeling of TNSA

Plasma expansion model: isothermal rarefaction wave solution "patched" at the ion front where quasi-neutrality breaks down

$$c_s = \left(\frac{ZT_e}{m_i}\right)^{1/2}, \quad u_f \equiv u_i(x_f) = c_s[2\ln(\omega_{pi}t)+1], \quad \mathscr{E}_{\max} = \frac{m_i}{2}u_f^2 \propto ZT_e$$

⚠: ion energy diverges due to infinite energy reservoir!
assume finite model (e.g thin foil expansion) with $T_e(t)$
assume finite acceleration time (extra patch)

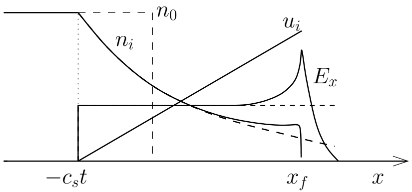

State of the art: "large" lasers

World records for energy cut-off, 2000-2016

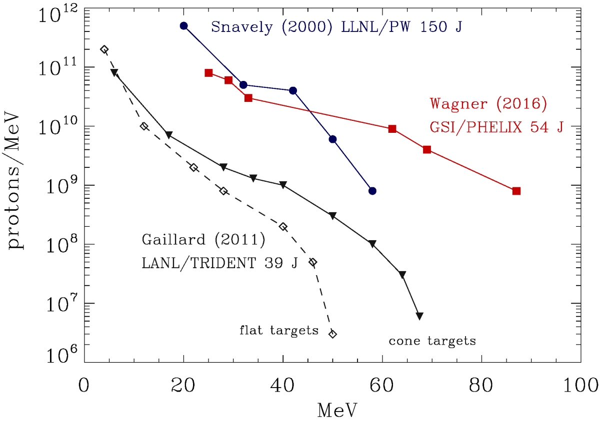

Values of laser pulse energy on target (typically <50% available) pulse duration 0.5-1 ps

State of the art: “small” lasers

Energy spectra and scaling of cut-off energy for fs laser pulses, <10 J in spot (selection of “close” experimental conditions)

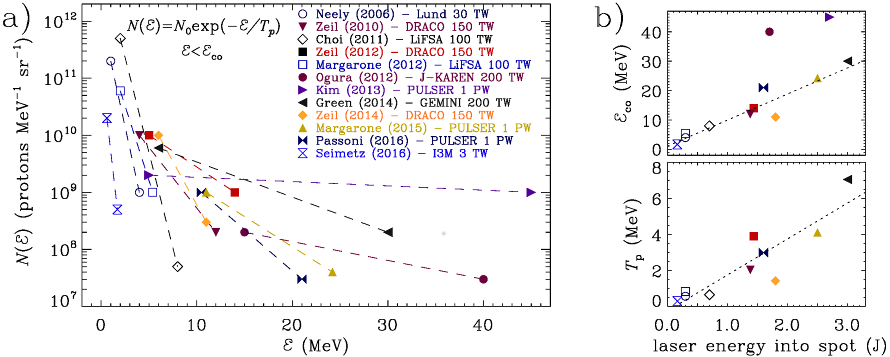

Almost linear scaling of proton energy with pulse energy/intensity (~ 9MeV/J)

Beyond TNSA: searching for other mechanisms

Unresolved issues and limitations of TNSA:

- broad ($\sim$ exponential) energy spectrum

$\rightarrow$ not suitable for most application

$\rightarrow$ hard to reach minimal requests for e.g. hadrontherapy (≥ 150 MeV)

- high repetition rate not easy with thin solid targets

Alternative regimes:

- Radiation Pressure Acceleration (RPA)
- Collisionless Shock Acceleration (CSA)

Early vision of radiation pressure acceleration (1966)

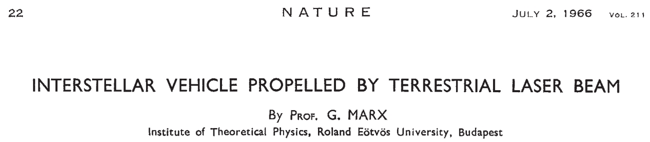
22 NATURE JULY 2, 1966 VOL. 211

INTERSTELLAR VEHICLE PROPELLED BY TERRESTRIAL LASER BEAM

By PROF. G. MARX

Institute of Theoretical Physics, Roland Eötvös University, Budapest

A solution to "Fermi's paradox": "*Laser propulsion from Earth . . . would solve the problem of acceleration but not of deceleration at arrival . . . no planet could be invaded by unexpected visitors from outer space*"

α-Centauri

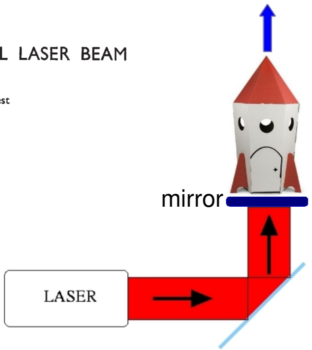

Starshot: laser-boosted light sails for space travel

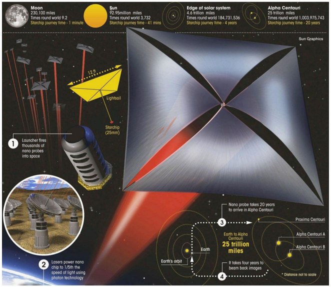

(credit: Breakthrough Starshot, breakthroughinitiatives.org)

Critical analysis: H. Milchberg, "Challenges abound for propelling interstellar probes", Physics Today, 26 April 2016

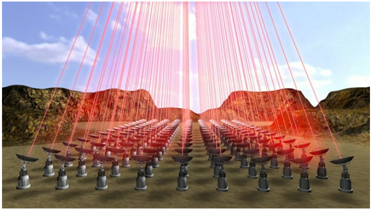

The accelerating mirror model of RPA

Perfect mirror boosted by a plane wave: momentum transfer (i.e. force) by light and mechanical efficiency η may be derived considering Doppler shifted reflection and number conservation of photons

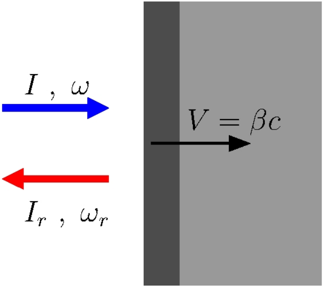

$$\frac{dp}{dt} = \frac{2I}{c}\frac{1-\beta}{1+\beta} \qquad \eta = \frac{2\beta}{1+\beta}$$

High efficiency ($\eta \to 1$) as $\beta \longrightarrow 1$

Light Sail motion

Mirror of finite mass in 1D:

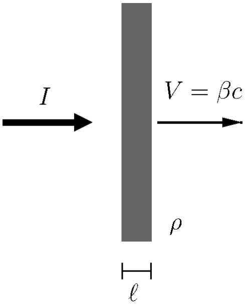

$$
\begin{aligned}
\rho \ell c \frac{d(\gamma\beta)}{dt} &= \frac{2}{c} I \frac{1-\beta}{1+\beta} \\
\mathscr{E}_{\text{max}} &= m_p c^2 (\gamma - 1) = m_p c^2 \frac{\mathscr{F}^2}{(2(\mathscr{F}+1))} \\
&\simeq m_p c^2 \mathscr{F}^2 / 2 \qquad (\mathscr{F} \ll 1\,,\ \beta \ll 1) \\
\mathscr{F} &= \frac{2}{(\rho\ell)} \int_0^\infty I(t')\,dt' \simeq \frac{2 I \tau_p}{\rho \ell}
\end{aligned}
$$

τ_p: pulse duration

Fast scaling with parameter $\mathscr{F}$
"rigid", coherent sail motion
$\longrightarrow$ **monoenergetic spectrum** for particles

Analogy with Acceleration by Thomson Scattering

Light Sail equations of motion have the same form as those of a particle undergoing Thomson Scattering
Landau & Lifshitz, *The Classical Theory of Fields*, ch.78 p.250 (1962).

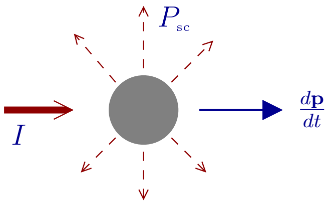

$$\frac{dp}{dt} = \sigma_T I \propto P_{sc}$$

Veksler's idea: coherent scattering by a cluster of radius $a \ll \lambda$ with N $(\gg 1)$ particles, $P_{sc} \to N^2 P_{sc} \Rightarrow \sigma_T \to N^2 \sigma_T$

How to make radiation pressure dominant?

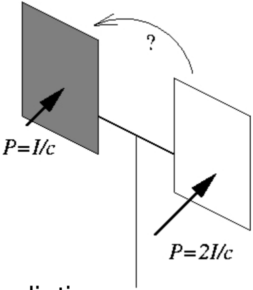

The "Optical Mill" rotates in the sense *opposite* to that suggested by the imbalance of radiation pressure: *thermal* pressure due to *heating* dominates

Dominance of radiation pressure ⟵ suppression of heating
Option for ultraintense lasers:
circular polarization
Macchi, Cattani, Liseykina, Cornolti, PRL **94** (2005) 165003

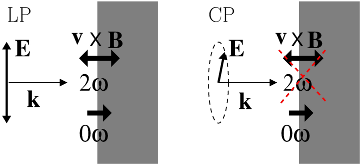

Evidence for $\mathscr{F}^2$ scaling (VULCAN)

Laser pulse: $t_p \simeq 800$ fs , $I = (0.5-3)\times 10^{20}$ W cm^{-2}
Target: $\sim (0.05-0.8)$ μm metal foils $\mathscr{F}_{\text{max}} \simeq 2 \times (Z/A)$

Spectral peaks with $\Delta\mathscr{E}/\mathscr{E} \simeq 20\%$ Energy/nucleon up to $\simeq 10$ MeV with $\mathscr{F}^2$-scaling on average

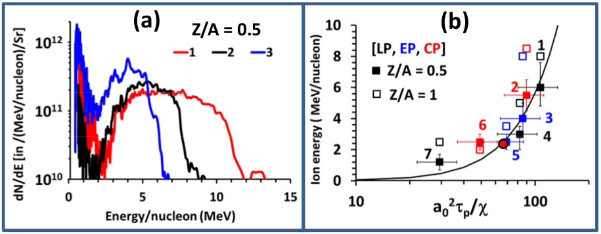

Broad spectra and weak dependence on polarization suggest important effects of target deformation for “long” pulse duration

S. Kar, K. F. Kakolee, B. Qiao, A. Macchi, M. Cerchez, D. Doria, M. Geissler, P. McKenna, D. Neely, J. Osterholz, R. Prasad, K. Quinn, B. Ramakrisna, G. Sarri, O. Willi, X. Y. Yuan, M. Zepf, M. Borghesi, PRL **109** (2012) 185006

Higher ion energy for circular polarization (GEMINI)

Laser pulse:

$t_p \simeq 45$ fs $I = 6 \times 10^{20}$ W cm^{-2}

Target: $10-100$ nm Carbon foils

$\mathscr{F}_{\text{max}} \simeq 1 \times (Z/A)$

Both proton and carbon energy higher for circular polarization (CP) than for linear (LP)

BUT maximum energy much less than theory: too much transmission through the foil

[C.Scullion, D.Doria, L.Romagnani, A.Sgattoni, K.Naughton, D.R.Symes, P.McKenna, A.Macchi, M.Zepf, S.Kar, and M.Borghesi, submitted]

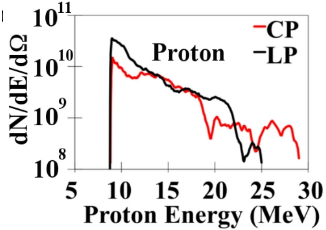

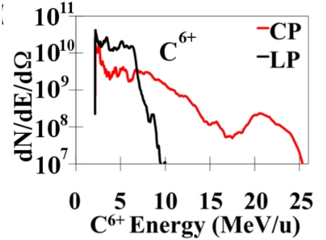

Collisionless Shock Acceleration

- Concept: shock wave of velocity $v_s = Mc_s$ ($M > 1$ Mach number, $c_s = \sqrt{ZT_e/Am_p}$ speed of sound) driven by the laser pulse into an ideal (collisionless) plasma (electric fields support the shock front rather than collisions)

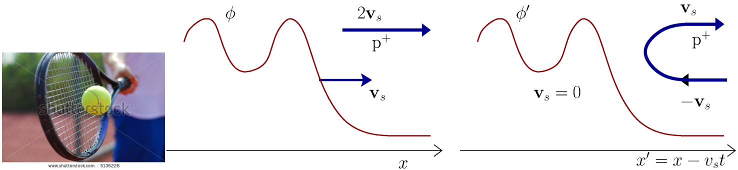

- Shock front is a moving potential barrier → "moving wall" reflection of some ions: $v_i \simeq 2v_s$

→ acceleration of monoenergetic, multi–MeV ions if v_s is constant and $T_e \simeq T_{\text{fast}} >$MeV

Laser-Driven Collisionless Shocks

Step 1:
- heating of "fast" electrons

Step 2:
- counterstreaming instabilities with "refluxing" electrons

OR

- radiation pressure acting as a "piston"

(Need to characterize optimal laser and target conditions)

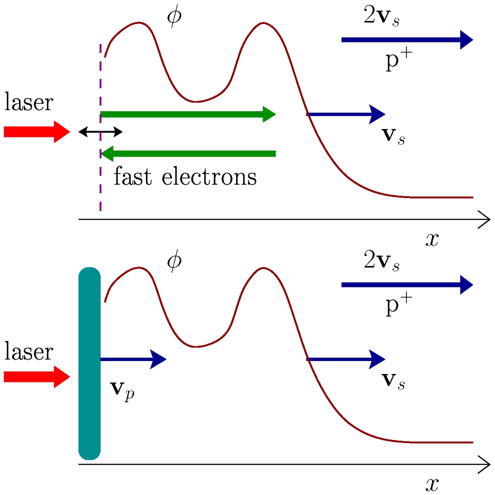

Monoenergetic CSA in CO_2 laser-H gas interaction?

UCLA experiment
Haberberger et al,
Nature Phys. **8** (2012) 95

Monoenergetic proton spectra:
$\mathcal{E}_{\text{max}} = 22$ MeV $\quad \Delta\mathcal{E} \lesssim 10^{-2}\mathcal{E}_{\text{peak}}$
Laser: 100 ps train of 3 ps pulses
$I = 6.5 \times 10^{16}$ W cm^{-2},
Target: H_2 gas jet
Interpretation: reflection from a shock driven by fast electrons

Number of protons is very low: is efficiency of CSA incompatible with monoenergetic spectra?

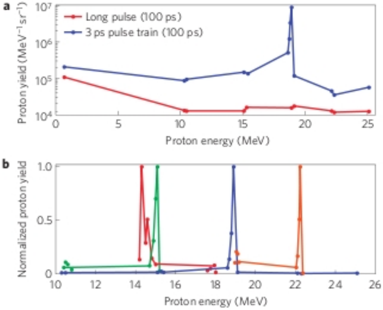

Figure 2 | Proton energy spectra. a, Proton spectra obtained with a 100-ps-long laser pulse (red) and a 100 ps macropulse consisting of a number of 3 ps micropulses (blue) both containing 60 J. The typical noise level on a single CR39 detector was 100 pits. The total number of protons contained within the monoenergetic peak was 2.5×10^5. **b**, The details of the energy spectra on four different laser shots with different macropulse structures (number of pulses and a_0 values ranging from 1.5 to 2.5).

Outlook and perspectives . . .

- Since 2000, progress in laser-driven ion acceleration has been obtained on various sides (cut-off energy, efficiency, energy spread . . .) in separate experiments with different mechanisms
- Laser-driven ion beams are already used for ultrafast plasma diagnostics and warm dense matter production
- Reaching required performance for other applications is still challenging:

- exploit new generation lasers (up to 10 PW power . . . and beyond?)
- develop and test alternative concepts
- “Have theory, will travel”

EXTRA SLIDES

Shock Loading and Energy Chirping (2D Simulation)

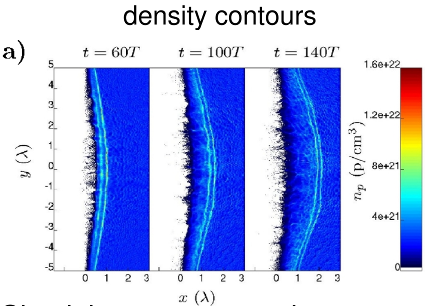

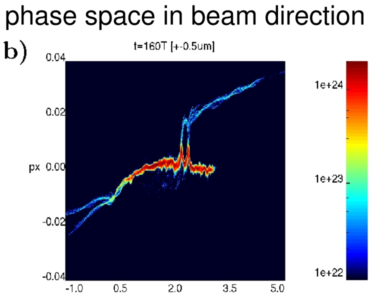

Shock loses energy to ions → v_s decreases → ions velocity ($2v_s$) decreases → spectrum broadens towards lower energies

Density profile and energy distribution of background ions are crucial for monoenergetic CSA (too many ions cannot be reflected anyway)

Macchi et al, PRE **85** (2012) 046402; Sgattoni et al, Proc. Spie **8779** (2013)

Proton probing of laser-plasma interactions

- charged beam:
  - field detection
- low emittance:
  - imaging capability
- laser driver:
  - easy synchronization
- broad spectrum:
  - time-of-flight arrangement
- short duration:
  - ultrafast resolution

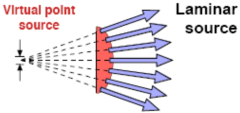

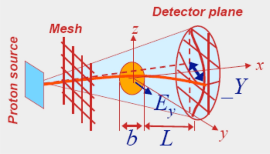

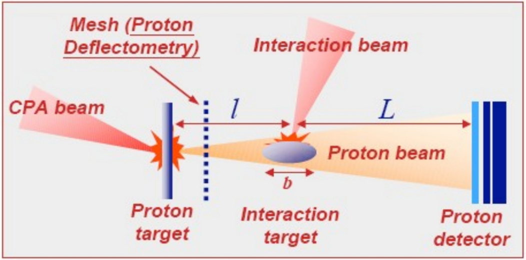

Achieving single-shot proton “movies”

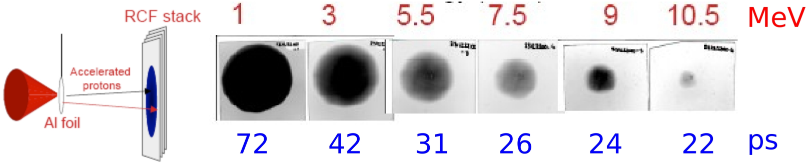

Radiochromic film (RCF) stack:
each layer a Bragg peak → a proton energy
Time-of-flight arrangement:
each layer → a probing time
(values refer to 1 mm flight distance)
Temporal resolution up to ~ 1 ps

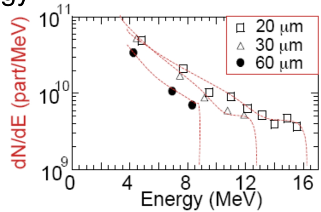

Proton "image" formation

Small angle deflections by $\mathbf{E}$ and $\mathbf{B}$ distributions create a density modulation δn on the RCF detector plane producing an "image" (with magnification M)

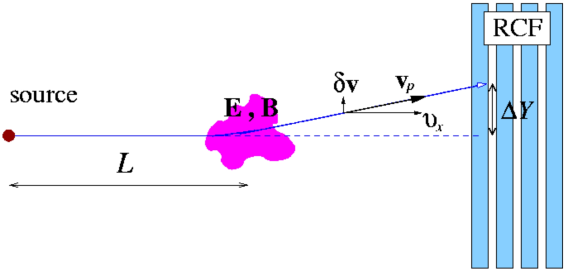

$$\Delta Y = |\delta \mathbf{v}|\Delta t \simeq \frac{eL}{2\mathcal{E}_p}\int (\mathbf{E}+\mathbf{v}_p\times\mathbf{B})_\perp dx$$

$$\frac{\delta n}{n_0} \simeq -\frac{1}{M}\nabla\cdot\Delta\mathbf{Y} \simeq \frac{-2\pi eLb}{\mathcal{E}_p M}\int_{-b/2}^{+b/2}\left(\rho - \frac{\mathbf{v}_p\cdot\mathbf{J}}{c^2}\right)dx$$

“Algorithm” for proton imaging analysis

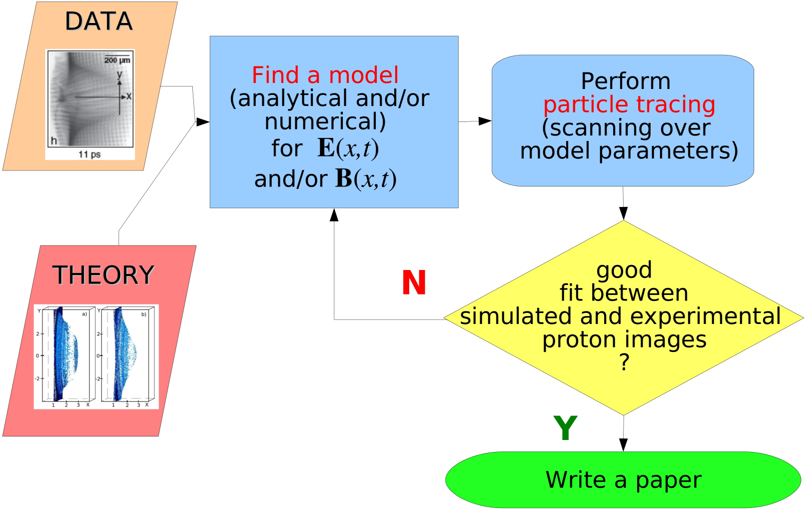

Probing proton acceleration with accelerated protons

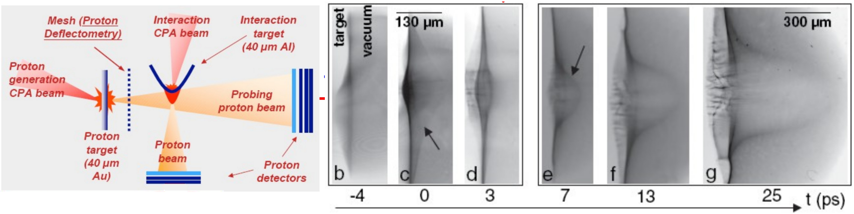

[L.Romagnani et al, Phys.Rev.Lett. **95** (2005) 195001]

Transverse probing of the target with a second proton beam: imaging of an expanding electric field front (bell-shaped contour) → confirmation that protons are accelerated at the rear surface of the target: TNSA (Target Normal Sheath Acceleration) model

Plasma Modeling: Maxwell-Vlasov Equations

$$\frac{df_a}{dt} = \frac{\partial f_a}{\partial t} + \frac{\partial}{\partial \mathbf{r}}(\dot{\mathbf{r}}_a f_a) + \frac{\partial}{\partial \mathbf{p}}(\dot{\mathbf{p}}_a f_a) = 0 \qquad f_a = f_a(\mathbf{r}, \mathbf{p}, t)$$

$$\dot{\mathbf{p}}_a = q_a(\mathbf{E} + \mathbf{v} \times \mathbf{B}) \qquad \dot{\mathbf{r}}_a = \frac{\mathbf{p}_a}{\sqrt{\mathbf{p}_a^2 + m_a^2}} \qquad \mathbf{v} = \frac{\mathbf{p}}{\sqrt{\mathbf{p}^2 + m_a^2}}$$

$$\rho(\mathbf{r}, t) = \sum_{a=e,i} q_a \int f_a d^3 p \qquad \mathbf{J}(\mathbf{r}, t) = \sum_{a=e,i} q_a \int \mathbf{v} f_a d^3 p$$

$$\nabla \cdot \mathbf{E} = \rho \qquad \nabla \cdot \mathbf{B} = 0 \qquad \nabla \times \mathbf{E} = -\partial_t \mathbf{B} \qquad \nabla \times \mathbf{B} = \mathbf{J} + \partial_t \mathbf{E}$$

Numerical solution: distribution function discretized over phase space trajectories of N particles (Particle-In-Cell method)

$$f_a(\mathbf{r}, \mathbf{p}, t) = \sum_{n=0}^{N-1} g(\mathbf{r} - \mathbf{r}_n(t))\delta(\mathbf{p} - \mathbf{p}_n(t)) \left\{ \begin{array}{l} d_t \mathbf{p}_n = q_a\left(\mathbf{E}(\mathbf{r}_n, t) + \mathbf{v}_n \times \mathbf{B}(\mathbf{r}_n, t)\right) \\ d_t \mathbf{r}_n = \mathbf{v}_n \end{array} \right.$$

Charging and "truncation" by electron escape

- An isolated, warm plasma in "real" 3D space gets charged due to the escape of $N_{\rm esc}$ electrons with energy $> U_{\rm esc}$ (since the binding potential is limited)
- For a simple spherical emitter of radius R having N_0 electrons at T_e:

$$N_{\rm esc} = N_0 \exp(-U_{\rm esc}/T_e) \qquad U_{esc} = e^2 N_{\rm esc}/R$$

- Message: cut-off energy $U_{\rm esc}$ (hence $\mathscr{E}_{\rm max}$) depends on target density, size, ...
- ⚠: the system is neither steady nor in Boltzmann equilibrium, the target is neither isolated nor grounded, ...

Some models fit better than others

Comparison of several models with experimental energies
[Perego et al, Nucl.Inst.Meth.Phys.Res.A **653** (2011) 89]

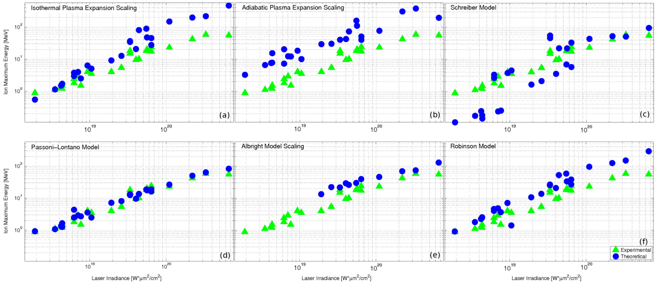

Fitting parameters: laser pulse energy, power, intensity, duration; fast electron energy, density, divergence; ion density and distribution; target thickness; . . . and various "phenomenological" quantities

Proton beam focusing and manipulation

TNSA-based "lenses" for spatial and spectral control of protons

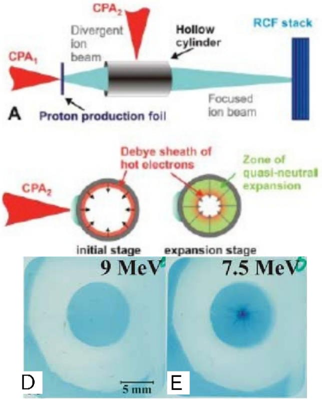

Toncian et al, Science **312** (2006) 410

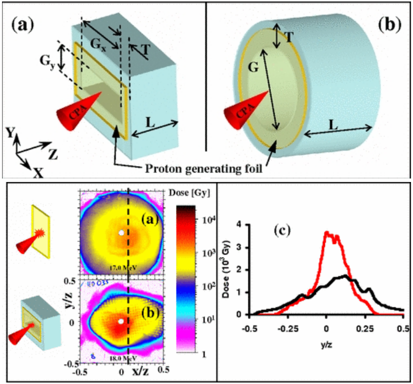

Kar et al, PRL **100** (2008) 105004

Engineering the initial distribution of ions

Hydrogen-rich microdot for monoenergetic acceleration

Use of *bacteria* as hydrogen-containing layer

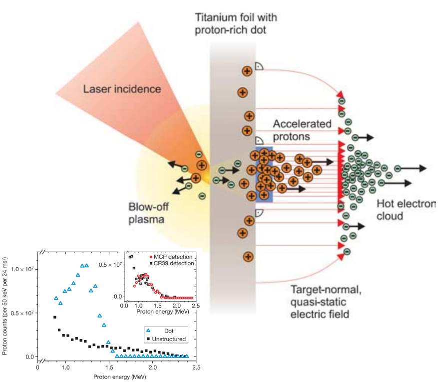

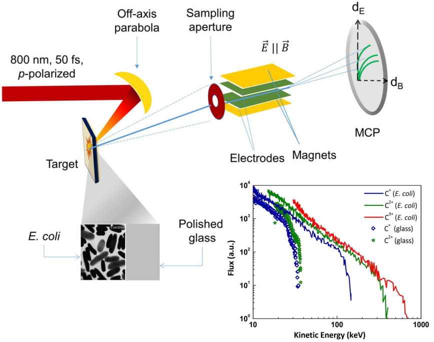

Schwoerer et al, Nature **439** (2006) 445

Dalui et al, Scient. Rep. **4** (2014) 1

Fast gain Light Sail in 3D

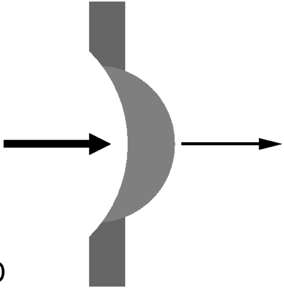

Transverse expansion of the target reduces on-axis surface density $\rho\ell$

$\Rightarrow$ *light sail gets "lighter"*:

boost of energy gain

at the expense of the number of ions

Faster gain $E_{\text{ion}}(t) \simeq \left(\frac{2It}{\rho\ell c^2}\right)^{3/5}$ predicted in 3D

[S.V.Bulanov et al, "Unlimited ion acceleration by radiation pressure", PRL **104** (2010) 135003]

Mechanism is effective for *relativistic* ions ($\mathscr{F} \gg 1$)

Need to explore this regime (relevant for ELI project) with fully 3D simulations over long time scales

High energy gain in 3D LS simulations

Laser: 24 fs, 4.8 μm spot, $I = 0.85 \times 10^{23}$ W cm^{-2} $\Longrightarrow$ **1.5 kJ**
Target: $d = 1$ μm foil, $n_e = 10^{23}$ cm^{-3}

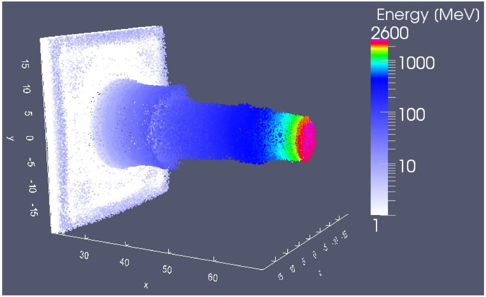

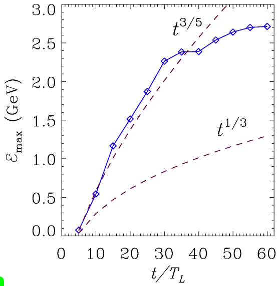

$\mathcal{E}_{max} \simeq 2.6$ GeV $>$ **4X 1D model prediction**
Macchi et al, Plasma Phys. Contr. Fus. **55** (2013) 124020;
Sgattoni et al, Appl. Phys. Lett. **105** (2014) 084105

3D simulation campaign: LSAIL project

(Large Simulations of ion Acceleration by Intense Lasers)

- PRACE award for access to FERMI BlueGene/Q at CINECA, Italy
- Typical set-up: 4096×1792^2 grid points, 2×10^{10} particles, 16384 cores used
- Particle-In-Cell (PIC) codes:

- ALADYN: C. Benedetti, A. Sgattoni, G. Turchetti, P. Londrillo, IEEE Trans. Plasma Science **36** (2008) 1790
- PICCANTE: Open Source code
  (L.Fedeli, A.Sgattoni, S.Sinigardi, et al)
  `github.com/ALaDyn/piccante`

Relativistic transparency and optimal thickness

Thin plasma foil becomes transparent because of relativistic effects when

$$a_0 > \zeta \equiv \pi \frac{n_e}{n_c} \frac{\ell}{\lambda} \qquad n_c = \frac{m_e \omega^2}{4\pi e^2} \text{ (cut-off density)}$$

→ optimal thickness as trade-off between reduced mass and transparency: $a_0 = \zeta$

- Diamond-Like Carbon ultrathin (nm) targets

→ avoid “prepulses” to cause early target disruption

- ultrahigh-contrast systems
- wide spots (and large energy), supergaussian intensity profiles to avoid strong deformation ?

High energy gain in 3D LS simulations (CH foil)

C+H double layer foil , $n_C = (64/6)n_c$, $n_H = 8n_c$

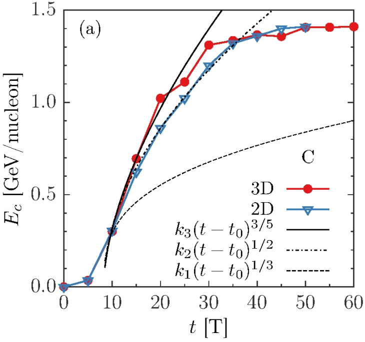

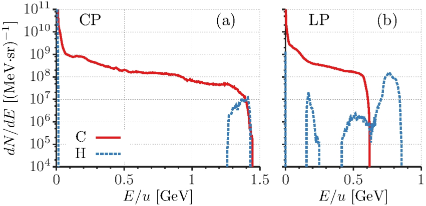

Circular vs Linear Polarization: Higher energy and narrower H spectrum for CP

Onset of transparency stops acceleration and is faster in 3D than in 2D → similar final energy in 2D and 3D (~1.4 GeV for CP)